Desalination and Water Treatment
www.deswater.com

doi: 10.5004/dwt.2023.29403

289 (2023) 248–257
March

Removal of textile dye Bemacid Red from water using *Casuarina equisetifolia* needles: kinetic and thermodynamic modeling

Souad Feddane, Khalil Oukebdane*, Mohamed Amine Didi*, Amel Didi, Afaf Amara, Oussama Larabi

Laboratory of Separation and Purification Technologies, Department of Chemistry, Faculty of Sciences, Box 119, University of Tlemcen 13000, Algeria, Tel.: +213659098692; emails: oukebdane.khalil@yahoo.fr (K. Oukebdane) ORCID-0000-0002-8537-4129, didiamel13@gmail.com (M.A. Didi) ORCID-0000-0002-7019-319X, feddanesouad13@gmail.com (S. Feddane) ORCID-0000-0001-5675-7609, amarafaf@yahoo.fr (A. Amara) ORCID-0000-0002-9000-5037, oussama_larabi@yahoo.fr (O. Larabi) ORCID-0000-0002-8064-5823

Received 28 September 2022; Accepted 22 February 2023

ABSTRACT

One of the principal tasks of modern industry is wastewater reuse. For this purpose, biosorbent are widely used; they are lignocellulosic-rich, sustainable material, low-cost and environmentally friendly materials. This study investigated the removal of a textile dye Bemacid Red (BR) using *Casuarina equisetifolia* needles (CEN) based on adsorption experiments. The biosorbent was characterized by the Fourier-transform infrared spectrum, scanning electron microscopy with energy-dispersive X-ray and pH_{pzc}. The kinetic, thermodynamic, and isotherms adsorption studies, also the effects of analytical parameters were investigated. The removal is fast and efficient; its efficiency exceeds 94%. The yield of BR removal increased with an increase in CEN dosage, initial dye concentration and ionic strength, but decreased with an increase in pH. The Sips model was selected as the most suited model to explain the BR adsorption onto CEN. The maximum adsorption capacity (Q_m) is 9.50 mg·g^{-1} according to monolayer adsorption. The BR adsorption was best described by pseudo-second-order kinetics. Thermodynamics studies showed that the adsorption system was spontaneous (ΔG = –1,276.35 J·mol^{-1}) and exothermic (ΔH = –11,074.24 J·mol^{-1}). The CEN makes it a suitable adsorbent for practical application and it can be exploited for the development of purification and extraction.

Keywords: Aqueous medium; Bemacid Red; *Casuarina equisetifolia*; Kinetic; Thermodynamics

1. Introduction

The dyes industry is a source of revenue for many countries in the world. With the advancement of society and technology, dyes are used in different industries like: pharmaceuticals, textiles, cosmetics, dyestuffs, food, etc [1]. The dyes are hazardous and very dangerous pollutants for the environment, especially after discharging into water sources without adequate and proper treatment, leading to environmental issues and serious threats to human life [2]. Textile industry is one of the most water-consuming industries that produce a large amount of colored waste, which is harmful to the environment. Since very little fresh water is available for human use (less than 3.5%), wastewater recycling and reuse technologies for the textile industry are essential. Many microorganisms are affected by the high toxicity of various pigments, which inhibit the growth of various animals in the aquatic ecosystem and reduce

* Corresponding authors.

the penetration of light into aquatic environments, inhibit photosynthesis and cause human toxicity to the kidneys, brain, and central nervous system while causing allergic, hemorrhagic, and carcinogenic effects. The dyeing process includes more than 100,000 synthetic dyes and many pigments that require large volumes of water. The washing step result in losses of the fixed dyes around 30%–70% and produce high volumes of contaminated effluents containing several dyes, which can be treated by several physical and chemical approaches [3]. The textile dye Bemacid Red (BR) is one of the most used textile dyes, mainly applied in the paper, textile, cosmetic, leather, plastic and pharmaceutical industries, etc [4].

Recently, adsorption has been the most commonly used technique to remove dyes from textile effluents due to advantages such as high efficiency, easy availability, simplicity and ease of processing as compared to other processes such as coagulation, membrane filtration, advanced oxidation, electro-chemical degradation, adsorption, Fenton process, photocatalytic degradation, phytoremediation, etc [5,6]. Therefore, low-cost, environmentally friendly and effective materials (so-called: biosorbents) such as: biochar [7], *Azolla pinnata* [8], different types of clay [9] are being developed.

Casuarina equisetifolia needles "CEN" is a widespread and evergreen tree, commonly known as ironwood, whistling pine, bulk oak and beefwood and it always grows in the coastal area. CEN is a nitrogen-fixing plant and has antimicrobial properties, contains tannins, triterpenes and proline, also various phytochemicals present in the plant include; ellagic acid, Gallic acid, quercetin, catechin [10]. It has been largely cultivated for coastal landscaping, agricultural promotion, as an ornamental shade tree and as firewood, or being planted as a wind-break [11]. The needles in the form of a decoction are used as a lotion for swelling and are also used in the treatment of coughs and ulcers. Seeds are antispasmodic, anthelmintic and antidiabetic. The phenolic compounds of the bark and needles have shown considerable antioxidant activity. Bark has activities like stomach ache, astringency, diarrhea, nervous disorders and dysentery. Extracts from the aerial parts and stem are reported to have angiotensin-converting enzyme inhibition activity. The extracts of leaves have anticancer properties and extracts from the fruit, stem and leaves have antimicrobial activity [11]. The dried CEN as high-availability biomass had been used in previous studies as an adsorbent [12–15].

This study is to evaluate the low-cost adsorbent CEN for BR dye removal from water. The kinetic, thermodynamic, isotherms batch adsorption experiment under various conditions studies and effects of analytical parameters were investigated. The adsorption process was then modeled using isotherm and kinetics models to predict the adsorption process. The physical and chemical characteristics of the CEN including pH_{pzc} and functional groups were determined. Adsorption isotherms were undertaken at 292 K to study the effects of solution: pH_i, ionic strength, temperature, time, stirring speed, adsorbent mass, initial dye concentration and particle size. Based on the modeling of the experimental data a mechanism of interaction between BR and CEN was proposed.

2. Methods

2.1. Chemicals and instrumentations

The BR dye (λ_{max} = 508 nm, $C_{24}H_{20}O_6S_2N_4NaCl$, M = 583 g·mol^{-1}, 98% purity) was obtained from the textile industry (SOITEX Tlemcen, Algeria) (Fig. 1). The initial pH was adjusted by using HNO_3 (69%) (AnalaR Normapur, VWR International, France) or NaOH (from CARLO ERBA Reagents, France) and measured pH with (Adwa AD1030 pH-meter model, Szeged, Hungary). The point of zero charge (pH_{pzc}) of the adsorbent was determined by the salt addition method using KNO_3 solution (0.1 mol·L^{-1}). Three different salts were used for the ionic strength effect: potassium nitrate KNO_3 (from Sigma-Aldrich, St-Quentin, France), sodium chloride NaCl (from Prolabo, Paris, France) and sodium sulfate Na_2SO_4 (from Sigma-Aldrich, St-Quentin, France). Magnetic stirrer (IKA-Werke magnetic stirrers with heating RT 10 P, Staufen, Germany) was used in extraction experiments, the BR dye concentration was determined at a wavelength of 508 nm using UV-Visible spectrophotometer SPECORD 210 plus (Analytik Jena, Jena, Germany) according to calibration curve obtained at the same conditions. The functional groups of the CEN were determined using Fourier-transform infrared spectroscopy (PerkinElmer Version 10.4.00, Waltham, Massachusetts, USA). The morphological analysis of adsorbent was carried out by HITACHI-SEM (TM1000, Hitachi Technologies, Pleasanton CA, USA) scanning electron microscope. The sample was coated with 15 nm gold and then analyzed under the microscope at an accelerating voltage of 20 kV. Centrifuge (SIGMA model 2-6, Goettingen, Germany) was used to accelerate the phase separation. Distilled water was used throughout experimental studies.

2.2. Adsorbent and dye preparation

The CEN was collected from Tlemcen region (Northwest of Algeria), it was first washed with distilled water to remove any dust particles, dried in an oven at 333 K for 24 h (until a constant weight was achieved), dried needles ware then blended and sieved to different sizes using laboratory sieve shaker (Orto Alresa). Fig. 2 shows the CEN grains used in this study. BR solution was prepared by dissolving an appropriate amount of BR powder in distilled water; the diluted solutions were prepared by suitable dilution of the stock solution.

2.3. Dye adsorption

The adsorption efficiency of the prepared adsorbent CEN was studied using an anionic BR dye. The studied adsorption parameters included initial pH from 2 to 9, adsorbent dose (m) from 0.001 to 0.100 g, adsorption time

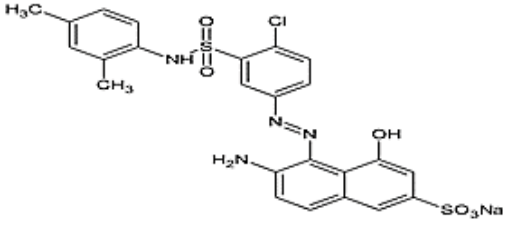

Fig. 1. Chemical structure of Bemacid Red dye.

from 2 to 300 min, initial dye concentration (C_0) from 5 to 100 ppm and adsorption temperature from 292 to 338 K. The adsorbent was put into 10 mL of dye solutions and the mixture was then agitated at 300 rpm for an equilibrium time. The effect of ionic strength was studied using three different salts: KNO_3, NaCl and Na_2SO_4 (0.1 to 2.5 mol·L^{-1}). The removal yield and adsorption capacity (amount of dye adsorbed per weight of adsorbent) at time, were evaluated using Eqs. (1) and (2), respectively [16]:

$$R(\%) = \frac{C_0 - C_e}{C_0} \times 100 \quad (1)$$

$$Q = \frac{(C_0 - C)V}{m} \quad (2)$$

where Q is the adsorption capacity (mg·g^{-1}), C_0 and C_e are respectively the initial and equilibrium concentrations of BR dye (ppm), V is the volume of the BR solution (L) and m is the weight of adsorbent (g).

3. Results and discussion

3.1. Characterization of adsorbent

The CEN surface morphology (Fig. 3) has shown a great irregularity surface and does not have large pores or cavities, which may be involved in the creation of the interaction interface with the BR dye molecules. Energy-dispersive X-ray spectroscopy (EDX) studies were carried out to determine the chemical composition of adsorbents. The corresponding EDX spectra showed carbon and oxygen to be the major constituents of raw CEN. The specific surface area was reported to be 351 m^2·g^{-1} [14].

Fig. 2. *Casuarina equisetifolia* needles grains.

Fourier-transform infrared spectroscopy (FTIR) was important to study the functional groups of CEN. The raw FTIR spectrum of CEN was represented in (Fig. 4). The broad absorption peak observed at 3,429 cm^{-1} corresponds to the stretching vibration of (–OH) group and (–NH) functional groups. The observed peak at 2,923 cm^{-1} may be attributed to alkyl (C–H) stretching vibrations. The characteristic (C=O) stretching is clearly seen at 1,731 cm^{-1} [17]. A peak at 1,627 cm^{-1} was due to carboxylate ions (–COO$^-$), a small peak observed at 1,451 cm^{-1} was attributed to (N–H) stretching vibrations of amine group, these carboxylate and amino groups might be part of the proline as one of the components of CEN as previously mentioned [18]. One other weak and the small peak at 1,317 cm^{-1} may be assigned to (C–O) stretching for alcohols or carboxylic acids and a stronger peak at 1,035 cm^{-1} might be attributed to (C–N) stretching of aliphatic amine. In the CEN spectra after treatment with BR, band shifts were observed at these peaks, indicating a possible involvement of these functional groups in the adsorption process. The presence of functional groups like acid, alcohol and amine is evident from these studies.

3.2. Determination of zero point charge (pH_{pzc})

Determination of the pH_{pzc} of an adsorbent is very important for adsorption studies, it is the pH value in which the positive and negative electrical charges found on the surface of the adsorbent are in equilibrium, these charges result from the adsorption of H_3O^+ and OH^- [19]. Below the pH_{pzc}, the surface of the adsorbent is positively charged and at higher pH levels than the pH_{pzc}, the surface is then negatively charged [20]. According to the results (Fig. 5), the pH_{pzc} value was equal to 5.0. Comparable results were found as: pH_{pzc} = 4.4 (Dahri et al. [12] and Kooh et al. [14]).

3.3. Effect of adsorption parameters

3.3.1. Effect of contact time

The removal of BR dye by the CEN was examined at different time intervals. Based on the result shown in Fig. 6,

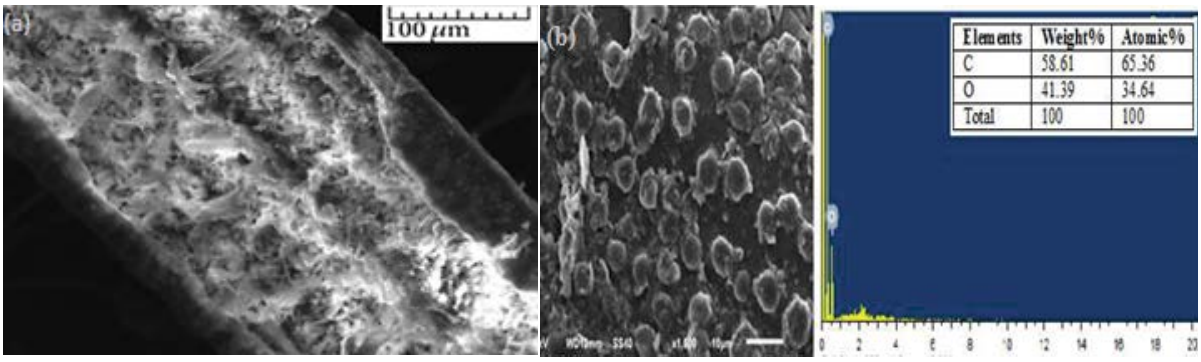

Fig. 3. (a) Scanning electron micrograph of *Casuarina equisetifolia* needles (100 μm) and (b) Scanning electron micrograph (10 μm) and energy-dispersive X-ray spectroscopy of *Casuarina equisetifolia* needles.

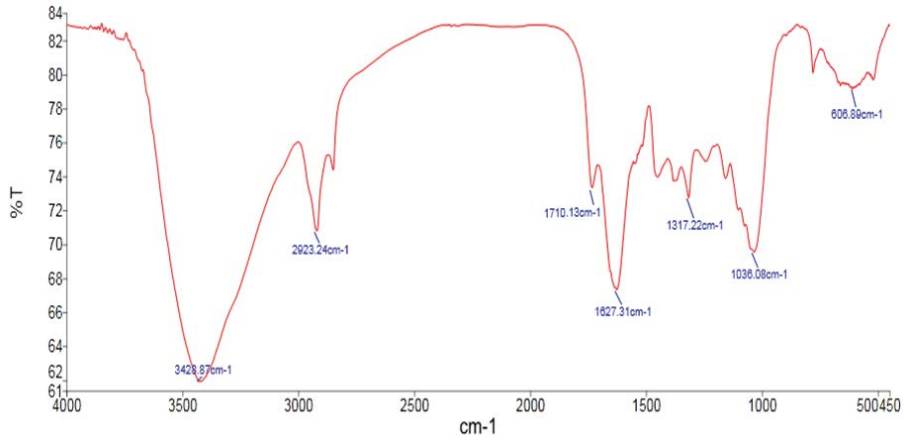

Fig. 4. Fourier-transform infrared spectra of *Casuarina equisetifolia* needles.

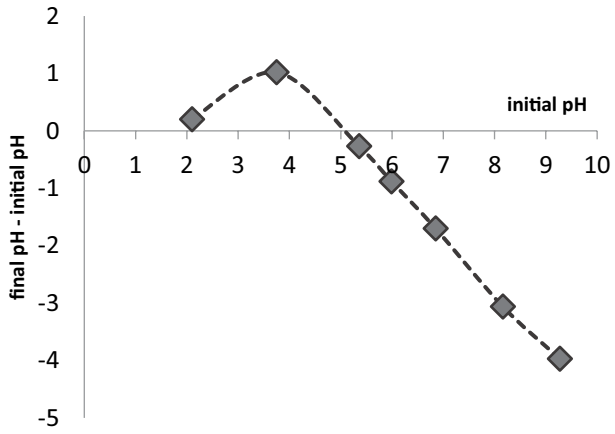

Fig. 5. pH of zero point charge of the *Casuarina equisetifolia* needles (pH_{pzc}). (m_{CEN} = 0.1 g; V = 50 mL; [KNO_3] = 0.1 mol·L^{-1}; T = 292 K; time = 24 h).

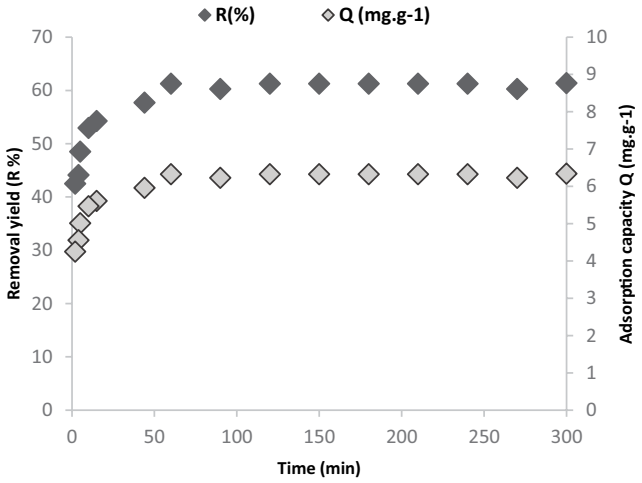

Fig. 6. Kinetic parameters for adsorption of Bemacid Red dye. ([BR] = 50 ppm; V = 10 mL; m_{CEN} = 0.05 g; T = 292 K; pH_i = 6.8; Φ = 300 rpm; d = 0.2 mm).

the yield of dye removal increases rapidly, the BR molecules easily gain accessibility to the sites in the first 5 min, the adsorption reaches 48%. The adsorption increases more rapidly during the initial time. This can be explained by the fact that a large number of active sites are available, resulting in the quick adsorption of BR dye onto the CEN surface. After that, the adsorption process becomes slower due to the gradual occupancy of these active sites on the adsorbent surface. At the later stage, these sites were reduced and repulsive forces may have started between the BR molecules on the CEN and aqueous phase [21,22]. At 60 min, the yield remains constant (Fig. 6). This may be caused by the fact that the active sites of adsorbent are already saturated.

3.3.2. pH effect on BR dye adsorption

The pH of the dye solution is an important parameter to be investigated and its value could greatly influence the adsorption since the H^+ and OH^- ions are adsorbed powerfully and it affects the ionic state of both the adsorbent and the dye [21,23]. The results shown in Fig. 7 indicate that

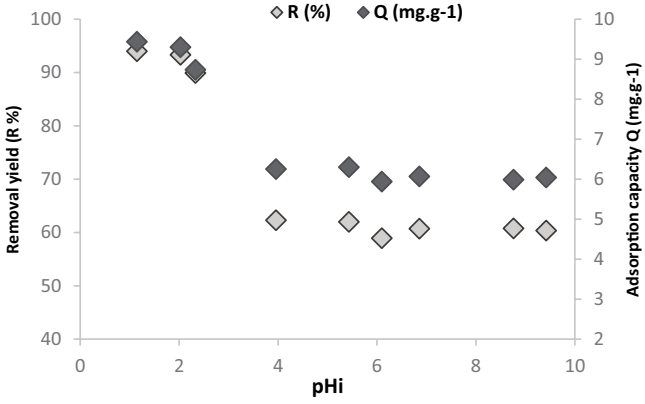

Fig. 7. pH effect on the adsorption of Bemacid Red dye using *Casuarina equisetifolia* needles adsorbent. ([BR] = 50 ppm; V = 10 mL; m_{CEN} = 0.05 g; T = 292 K; Φ = 300 rpm; d = 0.2 mm).

the adsorption of BR is very sensitive to changes in the initial pH of the dye solution.

The highest adsorption was observed in very acidic medium, the best removal yield (94%) was obtained at pH = 2, and the adsorption decreases with increasing pH up to pH = 4, and no further significant decrease was observed beyond pH = 5. To understand the effect of pH on the adsorption process, the point of zero charge (pH_{pzc}) of CEN was determined at 5 ± 0.1 by the salt addition method. At pH below pH_{pzc}, the CEN surface acquired positive charges and the higher BR dye removal in an acidic medium is mainly due to the electrostatic attraction between the positively charged surface of CEN and the BR negatively charged (sulfonate group SO_3^-). While in the basic medium, the BR removal is lower, this may be due to the competition of OH^- ions in solution with SO_3^- ions in the dye surface for the same active sites of the adsorbent; it suggests that the adsorption of BR onto CEN depends mainly on ionic interaction. The same observations are reported by Oukebdane et al. [22] for BR removal, and Kooh et al. [23] for another anionic dye removal.

3.3.3. Effect of adsorbent dosage and adsorbent particle sizes

The maximum dye removal yield (65%) was obtained using 0.100 g, while adsorption capacity decreased and reached the minimum value (3.23 mg·g^{-1}) (Fig. 8).

This was explained by the fact that with increasing dose, the available sites for adsorption also increased which led to the increase in adsorption yields, at higher adsorbent doses, reactive sites would be excessive to accommodate a given amount of dye molecules leaving most of the reactive sites unoccupied and therefore decrease of adsorption capacity [18].

Fig. 9 shows the effect of different ranges of adsorbent particle sizes (<0.2 mm, 0.2–0.25 mm, 0.25–0.4, 0.4–1 and >1 mm) on BR dye removal. The smallest particle size (<0.2 mm) yielded the highest yield dye removal at 60.5% (Q_e = 6.26 mg·g^{-1}), because it has a larger surface area to interact with dyes molecules compared to the bigger particle size. Thus, the removal yield decreases with increasing particle size [12]. The smallest particle size (<0.2 mm) was used for the rest of the experiment.

3.3.4. Effect of stirrer speed

Agitation is a classical parameter in adsorption phenomena; generally, it affects the distribution of the solute in the bulk solution and the formation of the outer boundary film [24]. Fig. 10 shows the BR dye adsorption by CEN at different stirring speeds ranging from 0 (without stirring) to 900 rpm.

The results show that a higher adsorption capacity was obtained for a stirring speed of 300 rpm. This agitation speed assures the diffusion of dye molecules onto the CEN adsorbent. For the experiment conducted without agitation, a significant reduction in the removal yield and capacity was noticed. When increasing the agitation speed to 300 rpm, the diffusion of dye molecules from the bulk liquid to the liquid boundary layer surrounding particles becomes higher because of the enhancement of turbulence and decrease of the thickness of the liquid boundary layer.

The insignificant effect of agitation for the 300–900 rpm range can be attributed to the high turbulence and decreasing thickness of the liquid boundary layer

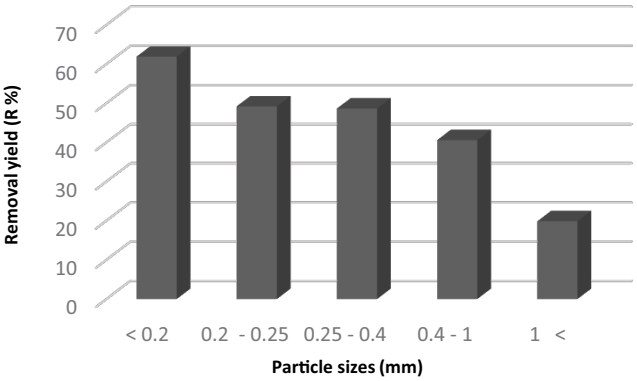

Fig. 9. Effect of different *Casuarina equisetifolia* needles particle sizes on Bemacid Red dye adsorption. ([BR] = 50 ppm; V = 10 mL; m_{CEN} = 0.05 g; T = 292 K; pH_i = 6.8; Φ = 300 rpm).

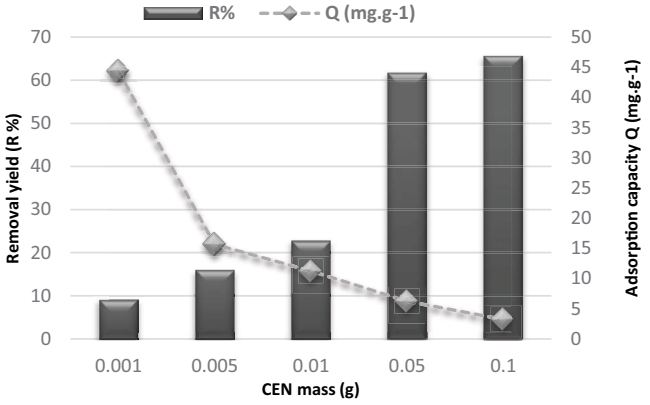

Fig. 8. Effect of *Casuarina equisetifolia* needles adsorbent dosage on Bemacid Red dye adsorption. ([BR] = 50 ppm; V = 10 mL; T = 292 K; pH_i = 6.8; Φ = 300 rpm; d = 0.2 mm).

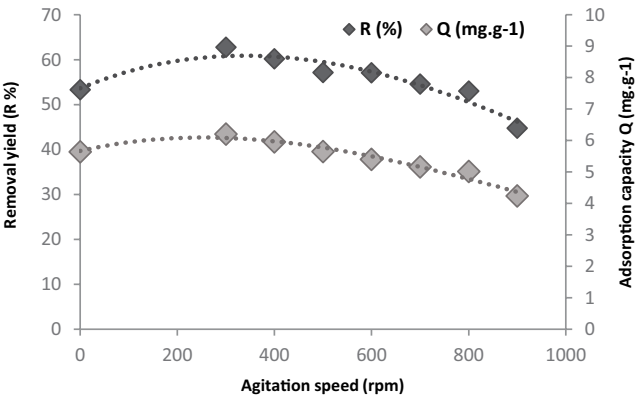

Fig. 10. Effect of stirring speed on Bemacid Red dye adsorption. ([BR] = 50 ppm; V = 10 mL; m_{CEN} = 0.05 g; T = 292 K; pH_i = 6.8; d = 0.2 mm).

around the adsorbent particles causing induction of system mobility [24].

3.3.5. Effect of ionic strength

The effect of ionic strength is important to verify the existence of the hydrophobic–hydrophobic interaction which is the attraction between the non-polar groups of the adsorbent and the non-polar group of the dye [14]. The effect of ionic strength on dye adsorption was studied at pH 6.8 (without adjustment), where both BR and CEN (pH_{pzc} = 5.0) were negatively charged, using various salt combinations (NaCl, KNO_3 and Na_2SO_4). When the electrostatic forces between the adsorbate and adsorbent surface are attractive, the adsorption capacity decreases with increasing ionic strength. Reversely, when the electrostatic forces are repulsive, the adsorption capacity increase with increasing ionic strength [25]. The data on the ionic strength effect follows this convention and are summarized in Fig. 11.

It can be observed that an increase in ionic strength of the solution led to higher adsorption as compared to a solution without salt addition, and the variation of salt concentration exhibits a major effect on BR dye adsorption. However, compared to the adsorption of other anionic dyes, this increase was stabilised at a salt concentration of 1 mol·L^{-1} for NaCl and KNO_3 and 0.5 mol·L^{-1} for (Na_2SO_4) [26,27]. In the present system, the main electrostatic interactions between the CEN surface and ionic compounds occur with cations, since the CEN surface is negative. The addition of cations allows the neutralization of the negative CEN sites, and the electrostatic repulsion barrier is therefore impeded and non-electrostatic interactions between the neutral CEN sites and the dye occur. These non-electrostatic interactions include H-bonds with low energy or short van der Waals interactions [27]. As the effluents of the textile industry have usually high salt content, this result suggests the practicality of using CEN in the remediation of the real situations.

3.3.6. Effect of the initial concentration

The effect of initial dye concentration was studied by varying concentrations from 5 to 100 ppm, which is shown in Fig. 12. A rapid increase in the removal yield of BR can be observed, and it is a function of the increase in the initial concentration. This trend gets closer to its maximal value in the order of 69.2% and then remains constant beyond the concentration 50 ppm (Q_e = 6.26 mg·g^{-1}). This is due to the saturation of CEN's active sites with the dye molecules and thus, the adsorption process slows down and finally reached equilibrium [12]. However, the adsorption capacity increases continuously reaching a maximum of 18.21 mg·g^{-1} for 100 ppm concentration value, this increase was caused by increasing in the number of the adsorbed dye molecules and thereby increasing the mass ratio of BR molecules to the fixed mass of CEN.

3.3.7. Effect of temperature

Fig. 13 shows the effect of temperature on the adsorption of BR onto CEN. It was observed that the removal yield and adsorption capacity slightly decreases with increasing temperature, indicating the exothermic nature of the adsorption process. An increase in temperature from 292 to 338 K decreased the dye removal yield from 57% to

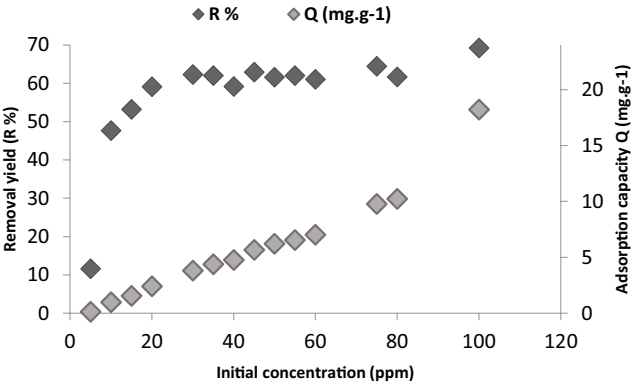

Fig. 12. Effect of the initial concentration on the adsorption of the Bemacid Red dye by *Casuarina equisetifolia* needles. (V = 10 mL; m_{CEN} = 0.05 g; T = 292 K; pH_i = 6.8; d = 0.2 mm; Φ = 300 rpm).

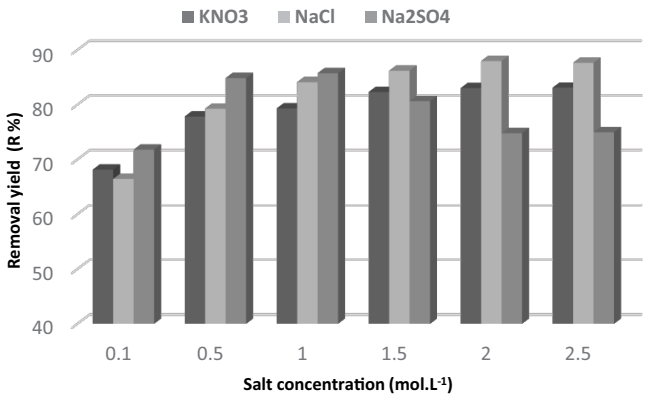

Fig. 11. Effect of ionic strength on Bemacid Red dye adsorption. ([BR] = 50 ppm; V = 10 mL; m_{CEN} = 0.05 g; T = 292 K; pH_i = 6.8; d = 0.2 mm; Φ = 300 rpm).

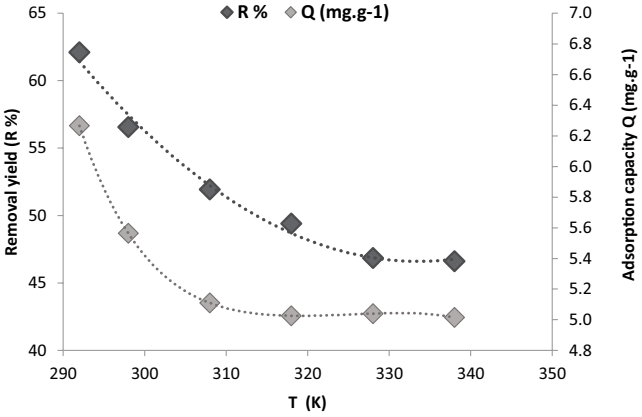

Fig. 13. Effect of temperature on Bemacid Red dye adsorption. ([BR] = 50 ppm; V = 10 mL; m_{CEN} = 0.05 g; pH_i = 6.8; d = 0.2 mm; Φ = 300 rpm).

46% and adsorption capacity from 6.26 to 5.01 mg·g^{-1}. This decrease in adsorption with increasing temperature may be due to the weakening of adsorptive forces between the active sites of CEN and BR molecules, additionally, this may be attributed to the escaping tendency of the BR from the solid phase to the bulk phase with the rise in temperature of the solution [24].

3.4. Equilibrium and kinetic study

The adsorption kinetics experiments for BR removal onto CEN adsorbent (0.05 g) have been conducted at the initial concentration dye of 50 ppm, in pH_i = 6.8 (without adjustment), at 292 K, varying contact times (2–300 min). The discoloration can be rapidly observed during the first 10 min, then the process continues slower, and the adsorption equilibrium occurs during 60 min. To better understand the adsorption kinetics behavior of BR onto the CEN adsorbent, the adsorption kinetics data have been considered using the four mentioned kinetics models (Table 1).

Where Q and Q_e are the adsorption capacities at any time and equilibrium (mg·g^{-1}), respectively; k_1 and k_2 are the pseudo-first-order adsorption rate constant and the pseudo-second-order adsorption rate constant, respectively, k_3 is the intraparticle diffusion rate constant, and C is the intercept; α (mg/(g·min)) is the constant initial adsorption rate, β (g·mg^{-1}) is the Elovich model constant.

The data of various kinetics models are summarized in Table 1. The correlation coefficient R^2, is higher for the pseudo-second-order (>0.99) than the pseudo-first-order, this shows that the pseudo-second-order model is more appropriate to the experimental data. This is further supported by the close values between the predicted Q_e values from pseudo-second-order model and the experimental Q_e, whereas the pseudo-first-order predicted Q_e values greatly deviated from experimental Q_e. According to Weber and Morris model, the plot of Q vs. $\sqrt{t}$ has to pass through the origin for intraparticle diffusion to be the limiting step. As shown in Table 1, C value was not equal to zero which indicates that the line does not pass through the origin which suggests that intraparticle diffusion is not the limiting step (with the involvement of other types of interactions). Based on the R^2 value, the Elovich equation was superior to the first-order equation and intraparticle diffusion model for the description of adsorption kinetics. However, the correlation coefficients corresponding to the pseudo-first-order, intraparticle diffusion and Elovich models are significantly lower than the pseudo-second-order, which means that none of these models is suitable to describe the adsorption of BR dye onto CEN and the adsorption process follows the pseudo-second-order model.

3.5. Study of adsorption isotherms

The adsorption isotherms are very important to describe adsorbate–adsorbent interaction [31]. To study the behavior of BR dye adsorption onto CEN, the Langmuir, Freundlich, Sips, Temkin and Dubinin–Radushkevich (D–R) isotherm models were applied to the experimental data at equilibrium state to be used for adsorption data modeling. The different parameters of the adsorption isotherms are reported in Table 2.

where K_L, K_F, K_T, K_{DR} and K_S are the adsorption constants for the Langmuir, Freundlich, Temkin, D–R and Sips models, respectively. C_e is the equilibrium dye concentration (ppm), Q is the adsorption capacity at different concentrations and Q_e is the adsorption capacity at equilibrium (mg·g^{-1}).

In the Freundlich equation "n" represents the empirical parameter that is related to the strength of the adsorption process. Constant B is related to the adsorption heat, R is the gas constant (8.314 J·K^{-1}·mol^{-1}), T denotes the absolute temperature in Kelvin and β gives the mean free energy of adsorption per molecule of the adsorbate. The $1/n$ is the Sips model exponent.

Based on R^2 values, the simulation of data was realized with the above five isotherm models. Temkin clearly indicates that this model does not fit with the experimental data (R^2 = 0.79), the Langmuir, Freundlich and D–R models gave higher R^2 values (0.98, 0.95, 0.98), respectively, they were ruled out due to the lower R^2 values.

The Sips isotherm model gave the higher R^2 value (R^2 = 0.99), is thus selected as the most suited model to explain the BR adsorption onto CEN. Sip's isotherm is a combination of both Langmuir and Freundlich expressions and is used for predicting heterogeneous adsorption systems; at lower BR concentrations, the model approaches Freundlich isotherm and for higher BR concentrations, it predicts a monolayer adsorption capacity characteristic of the Langmuir isotherm [33].

3.6. Thermodynamic study

The temperature effect on BR dye adsorption was studied by varying temperature from 292 to 338 K. It was found that

Table 1
Kinetic models equations, parameters and correlation coefficients

	Pseudo-first-order [28] [Eq. (3)]	Pseudo-second-order [28] [Eq. (4)]	Intraparticle diffusion [29] [Eq. (5)]	Elovich model [29,30] [Eq. (6)]
Equations	$\ln(Q_e - Q) = \ln Q_e - K_1 t$	$\frac{t}{Q} = \frac{1}{K_2 Q_e^2} + \frac{t}{Q_e}$	$Q = K_3\sqrt{t} + C$	$Q = \frac{1}{\beta}\ln(\alpha\beta) + \frac{1}{\beta}\ln(t)$
Parameters	K_1 = 0.003 Q_e (pred) = 1.77 Q_e (exp) = 6.33 R^2 = 0.558	K_2 = 0.109 Q_e (pred) = 6.36 Q_e (exp) = 6.33 R^2 = 0.999	K_3 = 0.121 C = 4.797 R^2 = 0.717	b = 2.40 α = 11569.2 t_0 (s) = 0.002 R^2 = 0.905

Table 2
Adsorption isotherms and parameters

Isotherm	Equation	Parameters
Langmuir [31]	$\frac{1}{Q}=\frac{1}{K_L Q_e C_e}+\frac{1}{Q_e}$ [Eq. (7)]	K_L (L·mg^{-1}) = 0.021 Q_m (mg·g^{-1}) = 9.50 R^2 = 0.98
Freundlich [18]	$\ln Q=\ln K_F+\frac{1}{n}\ln C_e$ [Eq. (8)]	n = 0.99 K_F (L·mg^{-1}) = 0.29 R^2 = 0.95
Temkin [18]	$Q_e=B\ln K_T C_e$ [Eq. (9)]	Δq (kJ·mol^{-1}) = 372.9 K_T (L·mg^{-1}) = 0.174 R^2 = 0.79
D–R [22]	$\ln Q=\ln q_m-K_{DR}\varepsilon^2$ [Eq. (10)] $\varepsilon=RT\ln\left(1+\frac{1}{C_e}\right)$ [Eq. (11)]	Q_m (mg·g^{-1}) = 7.53 K_{DR} (mol^2·kJ^{-2}) = 10.76 R^2 = 0.98
Sips [32]	$\ln\left(\frac{Q}{Q_e-Q}\right)=\frac{1}{n}\ln C_e+\ln K_s$ [Eq. (12)]	n = 0.61 K_S (L·mg^{-1}) = 0.005 R^2 = 0.99

Table 3
Thermodynamic parameters for Bemacid Red removal onto *Casuarina equisetifolia* needles

ΔH (J·mol^{-1})	ΔS (J·mol^{-1}·K^{-1})	ΔG (J·mol^{-1}) at T = 292 K
–11,074.24	–34.42	–1,276.35

adsorption decreased with temperature indicating the exothermic nature of the process. Thermodynamic parameters such as standard free energy change ($\Delta G°$) (kJ·mol^{-1}), entropy change ($\Delta S°$) (kJ·mol^{-1}·K^{-1}) and enthalpy change ($\Delta H°$) (kJ·mol^{-1}) were obtained from the following relations [18]:

$$K_c=\frac{C_{CEN}}{C_e} \tag{13}$$

$$\Delta G°=-RT\ln K_c=\Delta H°-T\Delta S° \tag{14}$$

$$\ln K_c=-\left(\frac{\Delta H°}{R}\right)\frac{1}{T}+\frac{1}{R}\Delta S° \tag{15}$$

where K_C is the equilibrium constant, C_{CEN} (mg·L^{-1}) and C_e (mg·L^{-1}) are the equilibrium dye concentrations on the adsorbent and in the solution, respectively, T (K) denotes absolute temperature and R (J·mol^{-1}·K^{-1}) is the universal gas constant. The values of ($\Delta H°$) and ($\Delta S°$) were calculated from their linear plots of lnK_C vs. 1/T. The values of the thermodynamic parameters obtained are reported in Table 3.

The negative value of ΔH suggested the adsorption process to be exothermic in nature; it was found –11.07 kJ·mol^{-1}. The value of standard change in free energy ($\Delta G°$) was found to be negative at T = 292 K, indicating the process spontaneity. The negative values of changes in entropy ($\Delta S°$) showed a decrease in randomness at the adsorbent-solution interface during the BR dye adsorption process on the CEN surface [14,22].

4. Conclusion

The study of BR dye removal onto CEN was investigated. For this, we developed the adsorption technique that represents a practical and environmentally friendly approach that satisfies the requirements of green chemistry by eliminating the use of conventional and expensive adsorbents and replacing them with this low-cost adsorbent. The discoloration can be rapidly observed during the first 10 min, then the process continues slower, and the adsorption equilibrium occurs during 60 min. The smallest particle size (<0.2 mm) gave the best dye removal yield. The effect of initial pH interestingly; the removal yield of BR dye was remarkably high at pH 2.0 where the anionic functionalities of CEN and BR were gradually neutralized by the excess H^+ ions. It was observed that an increase in ionic strength of the solution led to higher adsorption as compared to the solution without salt addition, and the variation of salt concentration exhibits a major effect on BR dye adsorption. The pseudo-second-order model is a better fit for the experimental data. The adsorption equilibrium data fitted well with the Sips isotherm model. The thermodynamic parameters of BR dye adsorption indicated that the adsorption is exothermic and spontaneous. The negative values of $\Delta S°$ showed a decrease in randomness at the adsorbent-solution interface during the BR dye adsorption process on the CEN surface. Indeed, under the experimental conditions used, the interactions involved in this case of adsorption would generally be between BR dye molecules and CEN surfaces via different possible interactions, mainly electrostatic attraction, ion exchange and complexation between BR and hydroxyl, amine and carboxyl groups. CEN used in this study is freely and abundantly available. It is clear that

the features of CEN make it a suitable adsorbent for practical application and it can be exploited for the development of extraction and purification.

Declaration

Conflict of interest

The author declares that there is no conflict of interest.

Funding

Not applicable.

Data availability statement

Data is contained within the article.

Acknowledgement

We gratefully acknowledge the DGRSDT Algeria for the financial support.

References

[1] X. Li, J. Li, W. Shi, J. Bao, X. Yang, A Fenton-like nanocatalyst based on easily separated magnetic nanorings for oxidation and degradation of dye pollutant, Materials, 13 (2020) 332, doi: 10.3390/ma13020332.
[2] M. Rastgordani, J. Zolgharnein, V. Mahdavi, Derivative spectrophotometry and multivariate optimization for simultaneous removal of Titan yellow and Bromophenol blue dyes using polyaniline@SiO_2 nanocomposite, Microchem. J., 155 (2020) 104717, doi: 10.1016/j.microc.2020.104717.
[3] P.R. de Souza, T.M. do Carmo Ribeiro, A.P. Lôbo, M.S. Tokumoto, R.M. de Jesus, I.P. Lôbo, Removal of bromophenol blue anionic dye from water using a modified exuviae of *Hermetia illucens* larvae as biosorbent, Environ. Monit. Assess., 192 (2020) 197, doi: 10.1007/s10661-020-8110-z.
[4] A. Gómez-Avilés, L. Sellaoui, M. Badawi, A. Bonilla-Petriciolet, J. Bedia, C. Belver, Simultaneous adsorption of acetaminophen, diclofenac and tetracycline by organo-sepiolite: experiments and statistical physics modelling, Chem. Eng. J., 404 (2021) 126601, doi: 10.1016/j.cej.2020.126601.
[5] M. Arbabi, N. Golshani, Removal of copper ions Cu(II) from industrial wastewater: a review of removal methods, Int. J. Epidemiol. Res., 3 (2016) 283–293.
[6] P. Senthil Kumar, G. Janet Joshiba, C.C. Femina, P. Varshini, S. Priyadharshini, M.S. Arun Karthick, R. Jothirani, A critical review on recent developments in the low-cost adsorption of dyes from wastewater, Desal. Water Treat., 172 (2019) 395–416.
[7] N. Suhaimi, M.R.R. Kooh, C.M. Lim, C.-T. Chou Chao, Y.-F. Chou Chau, A.H. Mahadi, H.-P. Chiang, N.H. Haji Hassan, R. Thotagamuge, The use of *Gigantochloa* bamboo-derived biochar for the removal of methylene blue from aqueous solution, Adsorpt. Sci. Technol., 2022 (2022) 8245797, doi: 10.1155/2022/8245797.
[8] M.R.R. Kooh, R. Thotagamuge, Y.-F.C. Chau, A.H. Mahadi, C.M. Lim, Machine learning approaches to predict adsorption capacity of *Azolla pinnata* in the removal of methylene blue, J. Taiwan Inst. Chem. Eng., 132 (2022) 104134, doi: 10.1016/j.jtice.2021.11.001.
[9] A.A. Adeyemo, I.O. Adeoye, O.S. Bello, Adsorption of dyes using different types of clay: a review, Appl. Water Sci., 7 (2017) 543–568.
[10] K. Dua, S. Nammi, D. Chang, D.K. Chellappan, G. Gupta, T. Collet, Medicinal Plants for Lung Diseases: A Pharmacological and Immunological Perspective, Springer, Singapore, 2021.
[11] O.U. Rao, M.C. Eswaraiah, M.C. Prabhakar, D. Santhikrupa, Hepatoprotective activity of aqueous extract from inflorescence and pollen grains of *Casuarina equisetifolia* against paracetamol induced hepatotoxicity in wistr rats, Int. J. Pharm. Sci. Res., 9 (2018) 743–747.
[12] M.K. Dahri, M.R.R. Kooh, L.B.L. Lim, Application of *Casuarina equisetifolia* needle for the removal of methylene blue and malachite green dyes from aqueous solution, Alexandria Eng. J., 54 (2015) 1253–1263.
[13] M. Abdullah, A.N.F. Azmi, M.Z.M. Azahar, F.N.M. Amri, K.A. Kadiran, D. Che Lat, H. Abu Kasim, A.H. Khalid, Application of *Casuarina equisetifolia* needle for the removal of heavy and light oil waste, AIP Conf. Proc., 2339 (2021) 020156, doi: 10.1063/5.0044212.
[14] M.R.R. Kooh, M.K. Dahri, L.B.L. Lim, C.A. Ng, The removal of rhodamine B dye from aqueous solution using *Casuarina equisetifolia* needles as adsorbent, Cogent Environ. Sci., 2 (2016) 1140553, doi: 10.1080/23311843.2016.1140553.
[15] S. Mohan, K. Sumitha, Removal of Cu(II) by adsorption using *Casuarina equisetifolia* bark, Environ. Eng. Sci., 25 (2008) 497–506.
[16] C. Hou, D. Zhao, S. Zhang, Y. Wang, Highly selective adsorption of Hg(II) by the monodisperse magnetic functional chitosan nano-biosorbent, Prog. Colloid Polym. Sci., 296 (2018) 547–555.
[17] M.K. Dahri, M.R.R. Kooh, L.B.L. Lim, Removal of Methyl violet 2B from aqueous solution using *Casuarina equisetifolia* needle, Int. Scholarly Sci. Not., 2013 (2013) 619819, doi: 10.1155/2013/619819.
[18] R. Khan Rao, A. Khatoon, Aluminate treated *Casuarina equisetifolia* leaves as potential adsorbent for sequestering Cu(II), Pb(II) and Ni(II) from aqueous solution, J. Cleaner Prod., 165 (2017) 1280–1295.
[19] K. Jafari, M. Heidari, O. Rahmanian, Wastewater treatment for Amoxicillin removal using magnetic adsorbent synthesized by ultrasound process, Ultrason. Sonochem., 45 (2018) 248–256.
[20] T.D. Çïftçï, Adsorption of Cu(II) on three adsorbents, Fe_3O_4/Ni/Ni_x B nanocomposite, carob (textit-*Ceratonia siliqua*), and grape seeds: a comparative study, Turk. J. Chem., 41 (2017) 760–772.
[21] V.P. Singh, Entropy Theory in Hydraulic Engineering: An Introduction, American Society of Civil Engineers, USA, 2014.
[22] K. Oukebdane, I.L. Necer, M.A. Didi, Binary comparative study adsorption of anionic and cationic azo-dyes on Fe_3O_4-bentonite magnetic nanocomposite: kinetics, equilibrium, mechanism and thermodynamic study, Silicon, 14 (2022) 9555–9568.
[23] M.R.R. Kooh, M.K. Dahri, L.B.L. Lim, L.H. Lim, C.M. Chan, Separation of acid blue 25 from aqueous solution using water lettuce and agro-wastes by batch adsorption studies, Appl. Water Sci., 8 (2018) 1–10.
[24] C. Djelloul, O. Hamdaoui, Removal of cationic dye from aqueous solution using melon peel as nonconventional low-cost sorbent, Desal. Water Treat., 52 (2014) 7701–7710.
[25] Y. Aldegs, M. Elbarghouthi, A. Elsheikh, G. Walker, Effect of solution pH, ionic strength, and temperature on adsorption behavior of reactive dyes on activated carbon, Dyes Pigm., 77 (2008) 16–23.
[26] N. Abidi, J. Duplay, A. Jada, E. Errais, M. Ghazi, K. Semhi, M. Trabelsi-Ayadi, Removal of anionic dye from textile industries effluents by using Tunisian clays as adsorbents. Zeta potential and streaming-induced potential measurements, C.R. Chim., 22 (2019) 113–125.
[27] A. Aguedach, S. Brosillon, J. Morvan, E.K. Lhadi, Influence of ionic strength in the adsorption and during photocatalysis of reactive black 5 azo dye on TiO_2 coated on non-woven paper with SiO_2 as a binder, J. Hazard. Mater., 150 (2008) 250–256.
[28] K.N.A. Putri, S. Kaewpichai, A. Keereerak, W. Chinpa, Facile green preparation of lignocellulosic biosorbent from lemongrass leaf for cationic dye adsorption, J. Polym. Environ., 29 (2021) 1681–1693.
[29] A.K. Nayak, A. Pal, Development and validation of an adsorption kinetic model at solid-liquid interface using normalized Gudermannian function, J. Mol. Liq., 276 (2019) 67–77.

[30] S. Das, S.K. Dash, K.M. Parida, Kinetics, isotherm, and thermodynamic study for ultrafast adsorption of azo dye by an efficient sorbent: ternary Mg/(Al + Fe) layered double hydroxides, ACS Omega, 3 (2018) 2532–2545.
[31] E.A. Dil, M. Ghaedi, A. Asfaram, S. Hajati, F. Mehrabi, A. Goudarzi, Preparation of nanomaterials for the ultrasound-enhanced removal of Pb^{2+} ions and malachite green dye: chemometric optimization and modeling, Ultrason. Sonochem., 34 (2017) 677–691.
[32] L.B.L. Lim, N. Priyantha, H.H. Cheng, N.A. Hazirah, Parkia speciosa (Petai) pod as a potential low-cost adsorbent for the removal of toxic crystal violet dye, Sci. Bruneiana, 15 (2016) 99–106.
[33] C.R. Girish, Various isotherm models for multicomponent adsorption: a review, Int. J. Civ. Eng. Technol., 8 (2017) 80–86.